

## New estimation of the spectral index of high-energy cosmic rays as determined by the Compton-Getting anisotropy

M. Amenomori,<sup>1</sup> X. J. Bi,<sup>2</sup> D. Chen,<sup>3</sup> S. W. Cui,<sup>4</sup> Danzengluobu,<sup>5</sup> L. K. Ding,<sup>2</sup>  
 X. H. Ding,<sup>5</sup> C. Fan,<sup>6</sup> C. F. Feng,<sup>6</sup> Zhaoyang Feng,<sup>2</sup> Z. Y. Feng,<sup>7</sup> X. Y. Gao,<sup>8</sup> Q. X. Geng,<sup>8</sup>  
 H. W. Guo,<sup>5</sup> H. H. He,<sup>2</sup> M. He,<sup>6</sup> K. Hibino,<sup>9</sup> N. Hotta,<sup>10</sup> Haibing Hu,<sup>5</sup> H. B. Hu,<sup>2</sup>  
 J. Huang,<sup>11</sup> Q. Huang,<sup>7</sup> H. Y. Jia,<sup>7</sup> F. Kajino,<sup>12</sup> K. Kasahara,<sup>13</sup> Y. Katayose,<sup>3</sup> C. Kato,<sup>14</sup>  
 K. Kawata,<sup>11</sup> Labaciren,<sup>5</sup> G. M. Le,<sup>15</sup> A. F. Li,<sup>6</sup> J. Y. Li,<sup>6</sup> Y.-Q. Lou,<sup>16</sup> H. Lu,<sup>2</sup> S. L. Lu,<sup>2</sup>  
 X. R. Meng,<sup>5</sup> K. Mizutani,<sup>13,17</sup> J. Mu,<sup>8</sup> K. Munakata,<sup>14</sup> A. Nagai,<sup>18</sup> H. Nanjo,<sup>1</sup>  
 M. Nishizawa,<sup>19</sup> M. Ohnishi,<sup>11</sup> I. Ohta,<sup>20</sup> H. Onuma,<sup>17</sup> T. Ouchi,<sup>9</sup> S. Ozawa,<sup>11</sup> J. R. Ren,<sup>2</sup>  
 T. Saito,<sup>21</sup> T. Y. Saito,<sup>22</sup> M. Sakata,<sup>12</sup> T. K. Sako,<sup>11</sup> M. Shibata,<sup>3</sup> A. Shiomi,<sup>9,11</sup> T. Shirai,<sup>9</sup>  
 H. Sugimoto,<sup>23</sup> M. Takita,<sup>11</sup> Y. H. Tan,<sup>2</sup> N. Tateyama,<sup>9</sup> S. Torii,<sup>13</sup> H. Tsuchiya,<sup>24</sup> S. Udo,<sup>11</sup>  
 B. Wang,<sup>8</sup> H. Wang,<sup>2</sup> X. Wang,<sup>11</sup> Y. Wang,<sup>2</sup> Y. G. Wang,<sup>6</sup> H. R. Wu,<sup>2</sup> L. Xue,<sup>6</sup>  
 Y. Yamamoto,<sup>12</sup> C. T. Yan,<sup>11</sup> X. C. Yang,<sup>8</sup> S. Yasue,<sup>25</sup> Z. H. Ye,<sup>15</sup> G. C. Yu,<sup>7</sup> A. F. Yuan,<sup>5</sup>  
 T. Yuda,<sup>9</sup> H. M. Zhang,<sup>2</sup> J. L. Zhang,<sup>2</sup> N. J. Zhang,<sup>6</sup> X. Y. Zhang,<sup>6</sup> Y. Zhang,<sup>2</sup> Yi Zhang,<sup>2</sup>  
 Zhaxisangzhu,<sup>5</sup> and X. X. Zhou<sup>7</sup>  
 (The Tibet AS $\gamma$  Collaboration)

<sup>1</sup>*Department of Physics, Hirosaki University, Hirosaki 036-8561, Japan*

<sup>2</sup>*Key Laboratory of Particle Astrophysics, Institute of High Energy Physics, Chinese Academy of Sciences, Beijing 100049, China*

<sup>3</sup>*Faculty of Engineering, Yokohama National University, Yokohama 240-8501, Japan*

<sup>4</sup>*Department of Physics, Hebei Normal University, Shijiazhuang 050016, China*

<sup>5</sup>*Department of Mathematics and Physics, Tibet University, Lhasa 850000, China*

<sup>6</sup>*Department of Physics, Shandong University, Jinan 250100, China*

<sup>7</sup>*Institute of Modern Physics, SouthWest Jiaotong University, Chengdu 610031, China*

<sup>8</sup>*Department of Physics, Yunnan University, Kunming 650091, China*

<sup>9</sup>*Faculty of Engineering, Kanagawa University, Yokohama 221-8686, Japan*

<sup>10</sup>*Faculty of Education, Utsunomiya University, Utsunomiya 321-8505, Japan*

<sup>11</sup>*Institute for Cosmic Ray Research, University of Tokyo, Kashiwa 277-8582, Japan*

<sup>12</sup>*Department of Physics, Konan University, Kobe 658-8501, Japan*

<sup>13</sup>*Research Institute for Science and Engineering, Waseda University, Tokyo 169-8555, Japan*

<sup>14</sup>*Department of Physics, Shinshu University, Matsumoto 390-8621, Japan*

<sup>15</sup>*Center of Space Science and Application Research, Chinese Academy of Sciences, Beijing 100080, China*

<sup>16</sup>*Physics Department and Tsinghua Center for Astrophysics, Tsinghua University, Beijing 100084, China*

<sup>17</sup>*Department of Physics, Saitama University, Saitama 338-8570, Japan*

<sup>18</sup>*Advanced Media Network Center, Utsunomiya University, Utsunomiya 321-8585, Japan*

<sup>19</sup>*National Institute of Informatics, Tokyo 101-8430, Japan*

<sup>20</sup>*Tochigi Study Center, University of the Air, Utsunomiya 321-0943, Japan*

<sup>21</sup>*Tokyo Metropolitan College of Industrial Technology, Tokyo 116-8523, Japan*

<sup>22</sup>*Max-Planck-Institut für Physik, München D-80805, Deutschland*

<sup>23</sup>*Shonan Institute of Technology, Fujisawa 251-8511, Japan*

<sup>24</sup>*RIKEN, Wako 351-0198, Japan*

<sup>25</sup>*School of General Education, Shinshu University, Matsumoto 390-8621, Japan*

## ABSTRACT

The amplitude of the Compton-Getting (CG) anisotropy contains the power-law index of the cosmic-ray energy spectrum. Based on this relation and using the Tibet air-shower array data, we measure the cosmic-ray spectral index to be  $-3.03 \pm 0.55_{stat} \pm < 0.62_{syst}$  between 6 TeV and 40 TeV, consistent with  $-2.7$  from direct energy spectrum measurements. Potentially, this CG anisotropy analysis can be utilized to confirm the astrophysical origin of the “knee” against models for non-standard hadronic interactions in the atmosphere.

*Subject headings:* cosmic rays — solar system: general

## 1. Introduction

The cosmic-ray (CR) energy spectrum has been observed using ground-based air shower detectors and various instruments on board satellites and balloons. It features a power law  $dN/dE \propto E^{-\gamma}$  in the energy range from 30 GeV to 100 EeV, where  $N$  denotes the number of cosmic rays at the top of the atmosphere,  $E$  the cosmic-ray particle energy. The spectral index  $\gamma$  changes from 2.7 to 3.1 around the “knee” at  $E \simeq 4$  PeV. Various models have been proposed for the origin of this knee; most models suppose that it is of astrophysical origin (Hörandel 2004), while there are some models that attribute it to non-standard high-energy nucleon interactions in the Earth’s atmosphere.

For a power-law CR energy spectrum, the Compton-Getting (CG) anisotropy involves the spectral index  $\gamma$ . When a detector observing cosmic rays moves relative to the rest frame of the CR plasma in the Earth orbit around the Sun, a fractional CR intensity variation  $\Delta I$  can be observed in the solar time frame. For a presumed power-law CR energy spectrum,

this CG anisotropy (Compton & Getting 1935; Gleeson & Axford 1968) is expressed as

$$\frac{\Delta I}{\langle I \rangle} = (\gamma + 2) \frac{v}{c} \cos \theta, \quad (1)$$

where  $I$  denotes the CR intensity,  $\gamma$  the power-law index of the cosmic-ray energy spectrum,  $v$  the orbital velocity,  $c$  the speed of light and  $\theta$  the angle between the arrival direction of CRs and the moving direction of the observer.

At multi-TeV energies, a clear evidence for the CG anisotropy in the solar diurnal variation was first reported in (Cutler & Groom 1986). The observed variation was in reasonable agreement with a sinusoidal curve expected from the CG anisotropy with the maximum phase of the curve deviating from 6:00 h by +2 hours at  $2\sigma$  significance. This deviation was ascribed to meteorological effects on the underground muon intensity. The Tibet air-shower experiment performed the first study on energy dependence of the solar diurnal variation and showed that it was consistent with the CG anisotropy above multi-TeV energies (Amenomori et al. 2004; Amenomori et al. 2006a).

Conventionally, the spectral index above  $\sim 100$  TeV is obtained by indirect measurements with air-shower arrays, in which each CR particle energy is determined from its shower size. The relation between particle energy and shower size is deduced from air-shower simulations assuming hadronic interaction models as a reasonable extrapolation of the accelerator results to the higher energy range. The spectral index thus obtained is valid only when no violation of the standard hadronic interaction is expected in the relevant energy range. This fact leaves a room for an argument whether the knee is due to non-standard high-energy nucleon interactions in the atmosphere or not.

On the other hand, the CG anisotropy does not depend on CR particle energy by Eq.(1). We can then measure the power-law index of the all-particle energy spectrum in the way it is virtually uninfluenced by hadronic interaction models, because air-shower simulations are used only for the purpose of estimating the rough energy range where we are observing the CG anisotropy. Potentially, this method makes it possible to confirm that the bend of the energy spectrum at the knee is of astrophysical origin, not due to non-standard hadronic interactions in the atmosphere.

## 2. Tibet Air-Shower Experiment

The Tibet air-shower experiment has been operating successfully at  $90.522^\circ$  E,  $30.102^\circ$  N and 4300 m above sea level since 1990. Being upgraded several times, the Tibet III array we use here was completed in November 1999 (Amenomori et al. 1992; Amenomori et al. 2002).

It consists of 533 scintillation counters of  $0.5 \text{ m}^2$  each. Each counter is viewed by a fast-timing (FT) photomultiplier tube and is placed on a  $7.5 \text{ m}$  square grid with an enclosed area of  $22,050 \text{ m}^2$  (Amenomori et al. 2003). A  $0.5 \text{ cm}$  thick lead plate is put on top of each counter to improve fast-timing data by converting gamma rays into electron-positron pairs. An event trigger signal is issued when any fourfold coincidence takes place in the FT counters recording more than  $0.6$  particle, which results in the trigger rate of about  $680 \text{ Hz}$  at a few-TeV threshold energy. We estimate the energy of a primary CR particle by  $\sum \rho_{\text{FT}}$ , which is the sum of the number of particles/ $\text{m}^2$  for each FT counter.

### 3. Cosmic-Ray Data Analysis

We collected  $7.7 \times 10^{10}$  events during 1319 live days from November 1999 to November 2005. After some data selections (i.e., software trigger condition of any fourfold coincidence in the FT counters recording more than  $0.8$  particle in charge, zenith angle of the arrival direction less than  $45^\circ$ , and air shower core position located in the array), the events left were histogrammed in hourly bins in the local solar time according to their event time and incident direction. To suppress the seasonal change in the daily variation, we corrected the number of events for each month considering monthly variations of the live time.

The daily and yearly event rates vary by  $\pm 2\%$  and  $\pm 5\%$  (Amenomori et al. 2003) respectively, affected mostly by meteorological effects. To remove these temporal variations, we adopted the following East–West subtraction procedure (Nagashima et al. 1989). We first obtain  $E(t)$  and  $W(t)$ , the daily variation at solar time frame for each of East and West incident events, according to the geographical longitude of incident direction of each event. Subsequently dividing  $E(t) - W(t)$  by  $2\delta t$ , an hour-angle separation between the mean directions of E- and W-incident events, we finally reach  $D(t)$ , the differential of the physical variation at solar time frame  $R(t)$ .

$$D(t) \equiv \frac{E(t) - W(t)}{2\delta t} = \frac{R(t + \delta t) - R(t - \delta t)}{2\delta t} = \frac{d}{dt}R(t) \quad (2)$$

The advantage of this method is that meteorological effects and possible detector biases which are expected to produce common variations for both E- and W-incident events largely cancel out.

#### 4. Results and Discussion

The CR events were divided into eight  $\sum \rho_{\text{FT}}$  bins in order to find out the energy region where the observed solar daily variation is free from effects other than the CG anisotropy. The fitting curve for the observed solar daily variation is expressed as

$$f(\lambda) = \alpha \cos\left(\frac{\pi}{12}(\lambda - \phi)\right), \quad (3)$$

where  $\alpha$  denotes the amplitude of the CG anisotropy,  $\lambda$  [hr] the local solar time and  $\phi$  [hr] the phase where the sinusoidal curve reaches its maximum. Note that in a differential form, the phase is shifted earlier by 6 hours (1/4 cycle) from the corresponding actual daily variation and the amplitude is  $\pi/12$  times that of the physical CG anisotropy.

Figure 1(a) shows  $\sum \rho_{\text{FT}}$  dependence of the phase  $\phi$  in Eq.(3). Although there exists deviation due to some contamination in the region of  $\sum \rho_{\text{FT}} < 50$ , the measured phase is consistent with the expected value of the CG anisotropy in  $\sum \rho_{\text{FT}} \geq 50$ . Therefore, we regard the observed variation in  $\sum \rho_{\text{FT}} \geq 50$  as caused by the CG anisotropy. Figure 1(b) shows  $\sum \rho_{\text{FT}}$  dependence of the observed amplitude  $\alpha$ . Since the CR energy spectrum in the multi-TeV region is expressed by a single power law, the amplitude should be consistent with a constant line if there is no contamination. This figure confirms that we do observe the CG anisotropy in the region of  $\sum \rho_{\text{FT}} \geq 50$ . Thus, we report here on the spectral index using  $9.7 \times 10^9$  events with  $\sum \rho_{\text{FT}} \geq 50$ . This region is roughly between 6 TeV and 40 TeV, corresponding to 20% and 80% of the median energy distribution, respectively.

Figure 2(a) shows the observed solar daily variation data fitted with a sinusoidal curve. The  $\chi^2$ -fitting results are summarized in Table I. From the amplitude of the solar daily variation, we obtained  $\gamma$  of CRs using the following relation,

$$\alpha = (\gamma + 2) \frac{v}{c} \frac{\pi}{12} F, \quad (4)$$

where  $\alpha$  denotes the amplitude,  $v = 2.978 \times 10^4$  [m/s] the average orbital velocity of the Earth and  $F = 0.827$  an effective geometrical factor by which  $\alpha$  decreases, calculated according to the latitude at Yangbajing site (see Appendix). The factor  $\pi/12$  emerges, because we measure the anisotropy in the differential form Eq.(2). As a result, we found  $\alpha = (10.9 \pm 1.2_{\text{stat}}) \times 10^{-5}$ . In Eq.(4), we omitted a minor correction. Strictly speaking, the orbital velocity of the Earth is time dependent. Although it varies  $\pm 2\%$ , we used the average  $v$  instead. It may become necessary to take this correction into account, when more data are accumulated.

A seasonal change of the sidereal daily variation due to the galactic anisotropy could produce a spurious variation in the solar time frame. The differential variation in the local extended-sidereal time (367.2422 cycles/yr) is shown in Figure 2(b). The insignificant variation in the extended-sidereal time  $(0.7 \pm 1.2_{\text{stat}}) \times 10^{-5}$  ensures that contamination in the solar

daily variation due to the seasonal change of the sidereal daily variation is less than 12% of the CG anisotropy. Adding this as a systematic error, we found  $\gamma = 3.08 \pm 0.55_{stat} \pm < 0.62_{syst}$ . This systematic error would become smaller in the future when more data are accumulated.

As the detection efficiency of the Tibet air-shower array depends on CR nuclei in this energy range (6 – 40 TeV), the correction for it should be taken into account. An air-shower simulation employing direct observational data for primary cosmic rays revealed that  $-0.05$  should be added to the  $\gamma$  above (Amenomori et al. 2006b). This correction is not needed, however, above  $\sim 60$  TeV where the detection efficiency becomes independent of nuclei, reaching  $\sim 100\%$ .

Finally, the spectral index  $\gamma$  between 6 and 40 TeV turned out to be  $3.03 \pm 0.55_{stat} \pm < 0.62_{syst}$ , consistent with 2.7 from direct energy spectrum measurements.

Using this CG anisotropy method, a future high-statistics experiment with a huge effective area will be able to measure the power-law index of the all-particle energy spectrum at higher energies. The spectral index  $\gamma$  measured by this method can be compared not only with those  $\gamma$  values by direct measurements below  $\sim 100$  TeV but also with those by indirect air-shower analyses above  $\sim 100$  TeV. This would check the mutual consistency between different ways to measure the CR energy spectrum. Following the same strategy, this CG anisotropy analysis can be applied to much higher energies to confirm the astrophysical origin of the knee.

The collaborative experiment of the Tibet Air Shower Arrays has been performed under the auspices of the Ministry of Science and Technology of China and the Ministry of Foreign Affairs of Japan. This work was supported in part by Grants-in-Aid for Scientific Research on Priority Areas (712) (MEXT), by the Japan Society for the Promotion of Science, by the National Natural Science Foundation of China, and by the Chinese Academy of Sciences.

## A. APPENDIX

Coefficient  $F$  in Eq.(4) is a correction factor for the latitude at Yangbajing site. To calculate  $F$ ,  $\cos \theta$  in Eq.(1) ( $\theta$ : the angle between the arrival direction of CRs and the moving direction of the observer) appears as

$$\begin{aligned} \cos \theta &= \cos L \cos \varphi \sin(\varphi + \psi) - \sin T \sin L \sin \varphi \\ &\quad - \cos T \cos L \sin \varphi \cos(\varphi + \psi) \end{aligned} \tag{A1}$$

with  $\psi = 2\pi t/24$ ,  $\varphi = 2\pi t/24/365.2422$ ,

where  $L = 30.102^\circ$  denotes the latitude at the Tibet air shower array,  $T = 23.44^\circ$  the tilt angle of the Earth's spin axis relative to the orbital axis,  $t$  [hr] the lapse time from the beginning of a year,  $\psi$  the solar time and  $\varphi$  a variable which advances from 0 to  $2\pi$  in a year. Suppose the Earth's spin axis were perpendicular to the ecliptic plane ( $T = 0^\circ$ ) for simplicity, Eq.(A1) would reduce to  $\cos \theta = \cos L \sin \psi$ . This means the amplitude of CG anisotropy decreases by a factor  $F = \cos L = 0.865$ . In reality, however, we need to take into account the tilt of the Earth's spin axis according to Eq.(A1). We found  $F = 0.827$ , approximately 4% smaller than 0.865, by numerically integrating Eq.(A1) so that  $\cos \theta$  can be expressed in terms of the solar time  $\psi$  only.

## REFERENCES

- Amenomori, M., et al. 1992, *Phys. Rev. Lett.*, 69, 2468
- Amenomori, M., et al. 2002, *ApJ*, 580, 887
- Amenomori, M., et al. 2003, *ApJ*, 598, 242
- Amenomori, M., et al. 2004, *Phys. Rev. Lett.*, 93, 061101
- Amenomori, M., et al. 2006a, *Science*, 314, 439
- Amenomori, M., et al. 2006b, *Advances in Space Research*, 37, 1932
- Compton, A. H., & Getting, I. A. 1935, *Phys. Ref.*, 47, 817
- Cutler, D. J., & Groom, D. E. 1986, *Nature (London)*, 322, 434
- Gleeson, L. J., & Axford, W. I. 1968, *Ap. Space Sci.*, 2, 431
- Hörandel, J. R. 2004, *Astropart. Phys.*, 21, 241
- Nagashima, K., et al. 1989, *Nuovo Cimento Soc. Ital Fis.*, 12C, 695



Table 1: The  $\chi^2$ -fitting results of the differential variation in the local solar time (a) and in the local extended-sidereal time (b), assuming the sinusoidal curve Eq.(3). The error bars are statistical only.

	$\alpha$ ( $\times 10^{-3}\%$ )	$\phi$ [hr]	$\chi^2/\text{d.o.f.}$
(a)	$10.9 \pm 1.2$	$-0.14 \pm 0.41$	8.03/22
(b)	$0.7 \pm 1.2$	$-4.0 \pm 6.9$	21.9/22

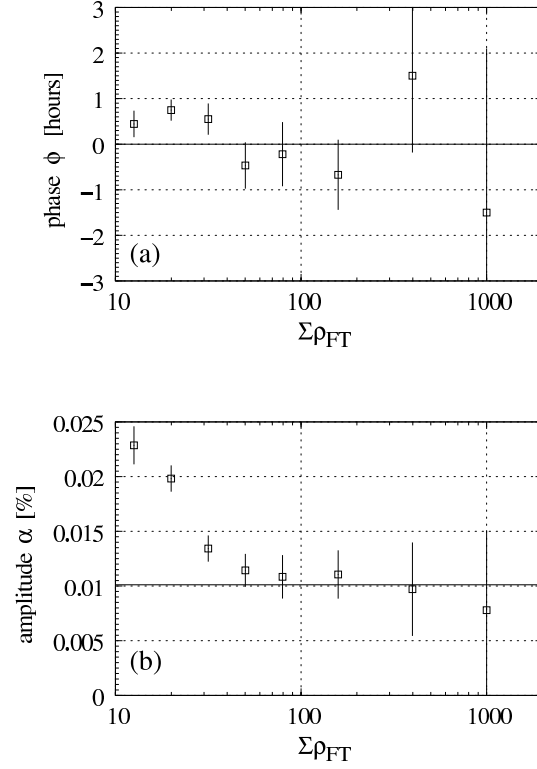


Fig. 1.— (a) :  $\Sigma\rho_{\text{FT}}$  dependence of the phase  $\phi$ , (b) :  $\Sigma\rho_{\text{FT}}$  dependence of the amplitude  $\alpha$ . Both are evaluated in a differential form. The solid lines show the expected values from the CG anisotropy, assuming  $\gamma = -2.7$ . The error bars are statistical only.

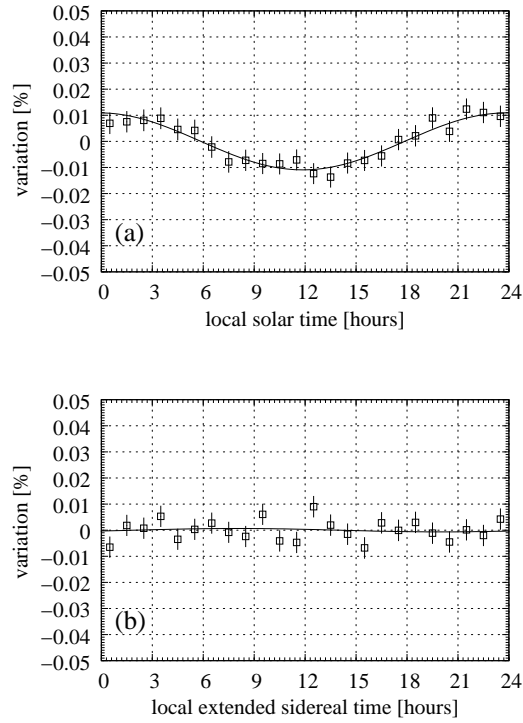


Fig. 2.— (a) : The differential variation of relative CR intensity in the local solar time  $D(t)$ , (b) : the differential variation of relative CR intensity in the local extended-sidereal time. The solid lines are the sinusoidal curves best fitted to the data. The error bars are statistical only.